



Published in final edited form as:

Obesity (Silver Spring). 2019 September ; 27(9): 1464–1471. doi:10.1002/oby.22558.

Elevated insulin and insulin resistance are associated with altered myelin in cognitively unimpaired middle-aged adults

J Patrick O’Grady¹, Douglas C Dean III², Kao Lee Yang¹, Cristybelles-Marie Canda¹, Siobhan M. Hoscheidt³, Erika J Starks¹, Andrew Merluzzi¹, Samuel Hurley^{5,6}, Nancy J Davenport^{1,4}, Ozioma C Okonkwo^{1,4}, Rozalyn M Anderson⁷, Sanjay Asthana^{1,4,7}, Sterling C Johnson^{1,4,7}, Andrew L Alexander², Barbara B Bendlin^{1,4}

¹Wisconsin Alzheimer’s Disease Research Center, University of Wisconsin School of Medicine and Public Health, Madison, WI, USA, 53792

²Waisman Center, University of Wisconsin Madison, Madison, WI, USA, 53705

³Stitch Center for Healthy Aging and Alzheimer’s Prevention, Wake Forest School of Medicine, Winston-Salem, NC, 27103

⁴Wisconsin Alzheimer’s Institute, University of Wisconsin School of Medicine and Public Health, Madison, WI, USA, 53726

⁵Neuroscience, University of Wisconsin Madison, Madison, WI, USA, 53705

⁶Radiology, University of Wisconsin Madison, Madison, WI, USA, 53792

⁷Geriatric Research Education and Clinical Center, Wm. S. Middleton Memorial VA Hospital, Madison WI, USA, 53705

Abstract

Objective—Insulin regulates metabolism and influences neural health. Insulin resistance (IR) and type II diabetes have been identified as risk factors for Alzheimer’s disease (AD). Evidence also suggests that myelinated white matter alterations may be involved in the pathophysiology of AD; however, it is unknown whether insulin or IR affect the underlying myelin microstructure. We examined the relationships between insulin, IR, and myelin, hypothesizing that IR would be associated with reduced myelin.

Methods—Cognitively unimpaired adults enriched for risk factors for AD underwent mcDESPOT imaging, a myelin sensitive neuroimaging technique. Linear regressions were used to test the relationship between HOMA-IR, insulin, and MWF, as well as interactions with *APOE* ϵ 4.

Results—Both IR and insulin level were associated with altered myelin content, wherein a significant negative association on MWF was observed in white matter regions and a positive association on MWF was observed in gray matter.

Send Correspondence to: Barbara B. Bendlin, PhD, J5/1M, Clinical Science Center, 600 Highland Ave, Madison, WI 53792, Phone: (608) 265-2483, bbb@medicine.wisc.edu.

Conflict of Interest Disclosures: The authors declare no conflict of interest.

Conclusion—The results suggest that insulin and IR influence white matter myelination in a cognitively unimpaired population. Additional studies are needed to determine the extent to which this may contribute to cognitive decline or vulnerability to neurodegenerative disease.

Keywords

Insulin resistance; magnetic resonance; imaging

INTRODUCTION

Increasing evidence suggests a pathophysiological link between Alzheimer's disease (AD) and type II diabetes. Individuals with type II diabetes have demonstrated significantly greater 20-year cognitive decline, a precursor to dementia, compared to individuals without type II diabetes.¹ Insulin resistance (IR), defined as an altered cellular and systemic response to insulin, is an early feature of type II diabetes, and a potential modifiable risk factor for AD.² IR has been associated with a higher risk of developing dementia due to AD³ and is associated with neurobiological alterations, including lowered regional glucose metabolism,⁴ higher amyloid burden,⁵ and AD pathology as measured in cerebrospinal fluid (CSF), as early as midlife.⁶ Previous data using diffusion imaging techniques further suggest type II diabetes and IR are associated with altered brain white matter.⁷ Given increasing evidence that alterations to oligodendrocytes,⁸ myelin,^{9, 10} and white matter in general,¹¹ may be associated with AD pathology, understanding the effect of insulin levels and IR on white matter microstructure is of particular importance.

Evidence from animal studies provide an underlying link between insulin signaling and the myelin sheath, a key constituent of the central nervous system's white matter. For example, insulin and insulin-like growth factor (IGF)-1 promote myelin producing oligodendrocytes during development.¹² Studies in insulin deficient mice models have reported a direct effect of insulin on the synthesis of brain cholesterol, a central element to myelin composition, where replenishing insulin restored cholesterol synthetic pathways in neurons and in glia.¹³ These data raise the notion that loss of insulin sensitivity may disrupt mechanisms of myelination, which in turn, may contribute or mediate vulnerability to neurodegenerative diseases, including AD.¹⁴

While prior studies have examined the effects of IR on diffusion imaging based measures, these metrics are non-specific to myelin.¹⁵ Myelin alterations have been observed in preclinical and clinical stages of AD,⁹ however, no studies to date have examined the association between IR and insulin and *in vivo* measures of brain myelin content. We aimed to fill this gap by examining the relationship between IR, insulin, and the myelin water fraction (MWF), a quantitative imaging measure of myelin content, using multicomponent driven equilibrium single pulse observation of T1 and T2 (mcDESPOT).¹⁶ We hypothesized that elevated insulin and IR would be negatively associated with mcDESPOT-derived MWF. A secondary aim of this study was to examine potential interactions between IR and *APOE* ϵ 4 carrier status. *APOE* ϵ 4 is a major susceptibility gene for late-onset AD and is reported to influence underlying brain metabolic and structural relationships¹⁷⁻¹⁸. We hypothesized that

negative associations between IR and MWF would differ between carriers and non-carriers of the *APOE* ϵ 4 allele.

METHODS

Experimental Design

Participants.—145 cognitively unimpaired late-middle-aged adults (mean age = 61.5 years [range = 45–74 years], 82 female / 44 male) were recruited into a brain imaging study from two ongoing longitudinal cohort studies, the Wisconsin Registry for Alzheimer's Prevention,¹⁹ and the Wisconsin Alzheimer's Disease Research Center (ADRC). Participants in these cohorts are enriched for parental history of AD. Inclusion criteria were: blood insulin and glucose levels available from prior fasting blood draw, mcDESPOT data, no self-reported history of diabetes diagnosis, in addition to no clinical diagnosis of a memory disorder or other major medical condition. Presence of type II diabetes was assessed by reviewing self-report diagnoses, usage of diabetes medication such as metformin or glipizide from self-reported medication records, and/or by using American Diabetes Association (ADA) criteria for type II diabetes.²⁰ Neuroimages and participant data were evaluated, and participants were excluded as outlined in Figure 1. Briefly, participants taking medications for diabetes (n=2); with a fasting blood glucose level more than three standard deviations above the mean (n=2); or with neuroimaging data that failed to register to the standardized template due to enlarged ventricles or motion artifacts (n=12), were excluded. One participant with fasting blood glucose of 127 mg/dL was retained in the analysis as they were not taking medication for type II diabetes.

The method for determining parental family history (FH), overnight fasting blood sample collection and processing, and height and weight recording have been previously described.⁶ To control for effects of body mass, we included "A Body Shape Index" (ABSI), which assesses body mass as calculated using waist circumference, body mass index (BMI), and height.²¹ *APOE* ϵ 4 genotype determination has been described previously.²² Genetic testing was performed at the Waisman Center at the University of Wisconsin-Madison, and participants were categorized as non-carriers (zero ϵ 4 alleles) or carriers (one or two ϵ 4 alleles). Participants also underwent neuropsychological assessment. The Mini-Mental State Examination (MMSE) was used to screen out participants with impaired cognition, using a cut score of 27.²³ Three participants were excluded from analyses based on a MMSE score lower than 27, resulting in a final sample of 126 participants (Table 1).

Calculations of IR and ABSI.—Insulin resistance was indexed by HOMA-IR [(glucose*insulin)/405] determined from fasting blood glucose and insulin levels. Body mass index (BMI) [weight in kilograms / height in meters²] was calculated and used to calculate ABSI [(waist circumference in meters) /BMI^{2/3} * height in meters^{1/2}].²¹

MRI Data Acquisition and Processing.—Participants underwent imaging on a 3T General Electric MR750 Discovery scanner (GE Healthcare, Waukesha, WI, USA) with an 8-channel receive-only head coil. mcDESPOT image acquisition (12 minutes total) consisted of spoiled gradient echo (SPGR) and balanced steady-state free precession (bSSFP) sequences acquired with eight flip angles.^{9,16} bSSFP images were acquired twice,

with and without radiofrequency phase cycling, for correction of magnetic field (B_0) inhomogeneities.²⁴ Actual Flip-angle Imaging (AFI) was acquired for correction of transmit field (B_1) inhomogeneities.²⁵ Images were acquired in the sagittal orientation, with a field of view of 25.6 cm by 25.6 cm by 16.8 cm and an isotropic voxel resolution of 2 mm. A high-resolution 3D Brain Volume Imaging (BRAVO) T1-weighted inversion-prepared sequence [repetition time (TR) = 8.1 ms, echo time (TE) = 3.2 ms, inversion time (TI) = 450 ms, flip angle = 12 degrees, field of view (FOV) = 256 mm, matrix = $256 \times 256 \times 156$, slice thickness = 1.0 mm], and a fluid-attenuated inversion recovery (FLAIR) sequence [TR=6000 ms, TE=123 ms, TI=1869 ms, flip angle=90 degrees, FOV = 256 mm, matrix = 256×256 , slice thickness = 2.0 mm] were also acquired to identify white matter hyperintensities (WMH).

SPGR and bSSFP data were fitted voxelwise to the mcDESPOT model using in-house software to estimate myelin water volume fraction (MWF), T1 and T2 of fast and slow-relaxing components, exchange rate, and the relative signal fraction of intra/extra-axonal water compartment.¹⁶ A third nonexchanging CSF compartment was included in the model to minimize the bias from CSF signal contamination.²⁶ Only MWF maps were considered in this study. The highest flip-angle SPGR image was aligned to the MNI (Montreal Neurological Institute) template using the Advanced Normalization Tools software.²⁷ This transformation was applied to each MWF map, aligning MWF to the MNI template. Registered MWF maps were smoothed using a 6mm full-width-at-half-max kernel.

White matter hyperintensity (WMH), presumed to be due to ischemia, may confound interpretation of mcDESPOT MWF results. Thus, WMH, as a ratio to total intracranial volume (ICV), was included as a covariate in all regression models. WMH segmentation was achieved using the T1-weighted BRAVO and T2-weighted FLAIR images and the Lesion Segmentation Toolbox version 1.2.2 in SPM8 (<http://www.fil.ion.ucl.ac.uk/spm/>).²⁸ Lesions were seeded based on spatial and intensity probabilities from the T1-weighted BRAVO images and hyperintense outliers on the T2-weighted FLAIR images, a method that has been validated with high agreement ($R^2 = 0.94$) to manual tracing.²⁸ ICV was calculated from T1-weighted BRAVO images using a “reverse brain masking” method. Using segmentation procedures in Statistical Parametric Mapping 12 (SPM12), gray, white, and CSF International Consortium for Brain Mapping (ICBM) probability maps were created and then summed to produce an ICV probability map. The inverse deformation field from unified segmentation was applied to the ICV probability map, to produce an ICV mask in native space. A threshold of 90% was applied to this participant-specific ICV probability map, and the total volume was extracted. WMH was divided by ICV and multiplied by 100 to give a ratio (WMHr) in units of percent of ICV and then log base 10 transformed.

Statistical Analysis.—Multiple voxelwise regression analysis using Statistical Parametric Mapping (SPM, Version 12) software was conducted to test for an association between IR and MWF. Further analyses explored the specific effect of insulin on MWF, as well as testing for potential interactions with *APOE* $\epsilon 4$ status. Covariates included age, sex, *APOE* $\epsilon 4$ status, ABSI, \log_{10} of WMHr, with predictors of interest either being IR, insulin, or *APOE* $\epsilon 4 \times$ IR. Monte Carlo simulations (AlphaSim, AFNI, <https://afni.nimh.nih.gov>) were performed to determine the minimum cluster-extent necessary for significance when correcting for multiple comparisons using the family-wise error rate (FWE) with a primary

voxel level threshold of $p < 0.005$. Contiguous clusters of a minimum extent of 174 voxels were determined to be significant ($p < 0.05$, corrected). An MRI Atlas of Human White Matter was used to identify regions of significant effect,²⁹ while SPM 12 was used to warp results to Montreal Neurological Institute (MNI) space for reporting. Multiple regression analyses were restricted to gray and white matter regions using a whole-brain mask.

RESULTS

Main effect of IR on MWF.

Voxelwise regressions between IR and MWF revealed widespread associations. Higher IR was associated with lower MWF in areas localized within areas of the deep white matter, including the parieto-occipital white matter, posterior thalamic radiation, superior occipital gyrus white matter and white matter of the cuneal cortex (see Figure 2 and Table 2). Higher IR was also associated with higher MWF in several cortical white matter regions (see Figure 2 and Table 2). Inspection of these results suggested that this effect may be due in part to participants with extreme IR; thus, we tested these associations in participants with IR less than 2 standard deviations of the mean ($n=121$). Similar to the previous analysis, higher IR was associated with higher MWF in fronto-temporal regions (Figure S1 and Table S1). Higher IR was also associated with lower MWF in parieto-occipital white matter (Figure S2 and Table S2), however, this cluster did not survive multiple comparison correction. Similar associations were observed between insulin concentration and MWF (see Figure 3 and Table 3).

APOE $\epsilon 4$ \times IR on MWF.

No significant *APOE* $\epsilon 4$ \times IR interactions on MWF were observed after correction for multiple comparisons. However, a notable uncorrected ($p < 0.05$) interaction within the middle frontal and precentral gyri and lateral occipital cortex was observed (Figure S2), suggesting *APOE* $\epsilon 4$ carriers may have a differential relationship between IR and MWF than non-carriers.

Hormone Therapy

Hormone therapy may impact brain structure and white matter.³⁰ In order to rule out potential confounds due to hormone therapy, a follow-up analysis to test whether insulin or IR differed among individuals on hormone therapy was performed. We found no difference in insulin and IR levels between participants on hormone therapy ($n=23$) versus those who were not on therapy ($n=103$) in our sample.

DISCUSSION

White matter alterations have been previously reported among individuals affected by type 2 diabetes,^{31–35} however, the effect of IR on myelin specifically has been unclear. In this study, we used a quantitative MRI technique known as mcDESPOT to examine the effect of IR on MWF, a neuroimaging proxy of myelin content, in a population of cognitively unimpaired middle-aged adults. Higher IR and insulin were observed to be associated with lower MWF in parieto-occipital white matter, posterior thalamic radiations, superior

occipital gyrus white matter and cuneus white matter, while higher IR and insulin were associated with higher MWF in several cortical regions, including frontal, parietal, and temporal cortices. This study is the first, to the best of our knowledge, to demonstrate insulin and IR to have a significant influence on the brain's myelin content and further complements an increasing literature that draws attention to the impact of insulin resistance on the brain in late-middle age.

The results of the present study align with previous findings using alternative neuroimaging techniques to assess the white matter microstructure. For example, previous studies using diffusion tensor imaging (DTI) have detected significant associations between IR and measures of white matter microstructure in cognitively unimpaired individuals, with decreased axial diffusivity observed in individuals with high HOMA-IR in parietal and temporal lobe white matter.³⁶ Though, mcDESPOT-derived MWF differ from measures of DTI, the negative associations between MWF and IR observed are consistent and complement with these results, suggesting that higher IR and insulin concentrations may contribute to underlying myelin microstructure alterations. Furthermore, positive associations observed in cortical brain regions, suggest that the effect of insulin and IR on cortical myelin may be different than the effect in deeper myelin rich brain regions.³⁷ Cortical gray matter contains a significant number of myelinated fibers, however, the composition of cortical myeloarchitecture differs to that of deep white matter, which may underlie this observed differential effect. Additionally, individuals with higher IR often have higher concentrations of insulin as the body produces more to combat the insulin resistance. As previously noted, insulin has been reported to promote myelin producing oligodendrocytes during development;¹² thus, we might speculate that higher insulin concentrations, as a result of higher IR, could foster myelination in some brain regions. Nevertheless, additional animal and human studies are necessary to further elucidate these neurobiological mechanisms.

Lower MWF in relation to higher insulin and IR were largely localized to posterior brain regions; while higher MWF in relation to higher insulin and IR were primarily observed in frontal, parietal, and temporal cortical brain regions (Figs 2 and 3). Posterior localization of white matter abnormalities have also been observed among individuals with mild cognitive impairment,³⁸ and other aging populations³⁹; while several of these regions have been previously been shown to be altered in type 2 diabetes.⁴⁰ We and others have also shown frontal and temporal white matter regions to exhibit extensive white matter alterations in aging populations⁹⁻¹¹, however, less is known about how myelinated fibers of these regions, particularly within the cortex, are affected by insulin and IR. While the results from the current study are in line with findings within the literature, our findings also suggest that myelin content in different brain regions may be differentially susceptible to the effects of insulin and IR. Importantly, while many of these brain regions are associated with the convergence of multimodal inputs and processing of memory, spatial, and semantic information,⁴¹⁻⁴² the functional significance of lower and/or higher MWF in these regions is unknown. The population evaluated here was cognitively unimpaired (MMSE score equal to or greater than 27,²³), and thus it is presently unclear whether the impact of IR or insulin on myelin has behavioral relevance or will contribute to vulnerability for neurodegenerative disease. Longitudinal follow-up is necessary to address this.

While the mechanisms by which IR and insulin impact myelin in humans are largely unknown, IR-induced alterations to cholesterol metabolism may be a possible mechanism behind the myelin changes observed in this study. Rodent studies directly link brain cholesterol synthesis to insulin-deficiency,¹³ and insulin has been shown to regulate activity of neuronal and glial sterol regulatory element-binding protein (SREBP)-2 activity,¹³ the transcription factor that regulates expression of genes involved in cholesterol synthesis. In the periphery, insulin is involved in stimulating the activity of 3-hydroxy-3-methylglutaryl-CoA reductase, an enzyme that helps in the synthesis of mevalonate, the rate-limiting step of cholesterol biosynthesis.⁴³ Data from this study indicate that myelin content is related to peripheral insulin sensitivity; however, additional studies are needed to link these findings to brain cholesterol synthesis.

Serum insulin and CSF insulin are positively correlated in normoglycemic subjects, however lower CSF insulin concentrations are observed among insulin-resistant subjects, suggesting altered transport of insulin across the blood-brain barrier in people with higher peripheral insulin resistance.³ Interestingly, patients with AD have lower CSF insulin levels, as well as higher plasma insulin levels compared to unimpaired controls.² Both insulin and IGFs receptors are expressed abundantly in the brain and relay signaling to a shared downstream intracellular pathway.¹² Ablation of the IGF-1 receptor gene in transgenic mice leads to deficiencies in myelination and a reduction in the populations of neurons.¹² Little is yet known about the effects of IR on brain myelin in humans *in vivo*, but these studies, taken together with our findings, suggest that peripheral IR is associated with myelin content. This in turn could negatively affect neural signaling and potentially contribute to axonal degeneration. Studies from our group suggest that IR is associated with neurodegeneration as shown on neuroimaging,⁷ and CSF biomarkers, particularly among *APOE* ϵ 4 carriers.⁶ Though an interaction between IR and *APOE* ϵ 4 genotype on MWF did not withstand correction for multiple comparisons, uncorrected interaction analyses suggest *APOE* ϵ 4 allele carrier status may be a contributing factor. Future studies with larger sample sizes may be informative for elucidating such interactions.

Multicomponent relaxometry techniques, such as mcDESPOT, are relatively new to the field and aim to decompose the measured MRI signal into contributions from discrete microstructural water compartments and quantify characteristics from these water pools, to provide a specific measure of myelin content. MWF estimates from mcDESPOT have been shown to provide sensitive measures of myelin content in a cuprizone mouse model,⁴⁴ track early myelin development in infants and children,¹⁷ and reveal myelin alterations in preclinical AD populations.⁹ While such studies give confidence that mcDESPOT is strongly sensitive, if not specific, to myelin content, future histological studies are critical for evaluating the microstructural imaging techniques. Furthermore, additional analyses combining MWF with other imaging measures, such as those acquired from DTI or magnetization transfer imaging (MTI), may provide greater insight about the relationship of myelin content to other microstructural changes that co-occur with changes to insulin sensitivity. Such investigations are likely to be beneficial for future investigations.

A few limitations deserve note. In our study, fasting glucose and insulin measurements were plasma based, and thus were indicative of peripheral IR, not a direct measurement of central

IR. Future studies will examine participants longitudinally to elucidate the temporal relationship between IR and myelin changes over time, especially in high risk subjects that have potential to go on to develop AD. Including participants with high IR yielded a significant effect of IR, but this effect was attenuated when examining more moderate levels of IR. It's possible that there is a threshold at which negative impacts are observed, or possibly that those individuals with the highest IR have also had a longer duration of metabolic dysregulation. Another important consideration will be to incorporate histopathological and immunohistochemical methods to quantify white matter in post-mortem analyses.⁴⁵ A noteworthy model of myelin involvement in AD pathogenesis highlights the observation that medications targeting type II diabetes may have myelin protecting effects, which in turn may translate into efficacy in some neurodegenerative diseases including AD.¹⁰

Supplementary Material

Refer to Web version on PubMed Central for supplementary material.

ACKNOWLEDGEMENTS

Sincere thanks to colleagues from the Wisconsin Alzheimer's Disease Research Center and Wisconsin Registry for Alzheimer's Prevention, including Charles Illingworth, Jen Oh, Vince Pozorski, Kelsey Melah, Nicholas Vanderwerker, and especially the late Jitka Sojkova. And finally, thanks to our dedicated participants because without them this project would not be possible.

Funding: Support for this project was provided by the National Institute of Aging (R01 AG037639 [BBB], R01 AG027161 SCJ) and ADRC P50 AG033514 (SA and BBB - Project 2). DCD is supported by a career development award provided by the National Institutes of Mental Health (K99MH110596).

REFERENCES

1. Rawlings AM, Sharrett AR, Schneider ALC, Coresh J, Albert M, Couper D, Griswold M, Gottesman RF, Wagenknecht LE, Windham BG, Selvin E (2014) Diabetes in midlife and cognitive change over 20 years: the atherosclerosis risk in communities neurocognitive study. *Annals of Internal Medicine*, 161(11), 785–93 [PubMed: 25437406]
2. Watson GS, Craft S (2003) The role of insulin resistance in the pathogenesis of Alzheimer's disease. *CNS Drugs*, 17(1), 27–45 [PubMed: 12467491]
3. Craft S (2007) Insulin resistance and Alzheimer's disease pathogenesis: potential mechanisms and implications for treatment. *Curr Alzheimer Res*, 4(2), 147–152 [PubMed: 17430239]
4. Willette A, Bendlin BB, Starks EJ, Birdsill AC, Johnson SC, Christian BT, Okonkwo OC, La Rue A, Hermann BP, Kosciak RL, Jonaitis EM, Sager MA, Asthana S (2015) Association of Insulin Resistance With Cerebral Glucose Uptake in Late Middle-Aged Adults at Risk for Alzheimer Disease. *JAMA Neurology*, 72(9), 1013–20. [PubMed: 26214150]
5. Willette A, Johnson SC, Birdsill AC, Sager MA, Christian B, Baker LD, Craft S, Oh J, Statz E, Hermann BP, Jonaitis EM, Kosciak RL, La Rue A, Asthana S, Bendlin BB (2015) Insulin resistance predicts brain amyloid deposition in late middle-aged adults. *Alzheimer's and Dementia*, 11 (5), 504–510.
6. Starks EJ, O'Grady JP, Hoscheidt SM, Racine AM, Carlsson CM, Zetterberg H, Bendlin BB (2015) Insulin Resistance is Associated with Higher Cerebrospinal Fluid Tau Levels in Asymptomatic *APOE* epsilon4 Carriers. *J Alzheimers Dis*, 46(2), 525–533 [PubMed: 25812851]
7. Xie Y, Zhang Y, Qin W, Lu S, Ni C, Zhang Q (2016) White matter microstructural abnormalities in type 2 diabetes mellitus: a diffusional kurtosis imaging analysis. *AJNR Am J Neuroradiol*, 38(3), 617–625 [PubMed: 27979796]

8. Braak H, Del Tredici K (2015) The preclinical phase of the pathological process underlying sporadic Alzheimer's disease. *Brain*, 138, 2814–2833 [PubMed: 26283673]
9. Dean DC III, Hurley SA, Kecskemeti SR, O'Grady JP, Canda C, Davenport-Sis NJ, Carlsson CM, Zetterberg H, Blennow K, Asthana S, Sager MA, Johnson SC, Alexander AL, Bendlin BB (2017) Association of Amyloid Pathology With Myelin Alteration in Preclinical Alzheimer Disease. *JAMA Neurology*, 74(1), 41–49 [PubMed: 27842175]
10. Bartzokis G (2011) Alzheimer's disease as homeostatic responses to age-related myelin breakdown. *Neurobiology of Aging*, 32(8), 1341–1371 [PubMed: 19775776]
11. Bendlin BB, Carlsson CM, Johnson SC, Zetterberg H, Blennow K, Wllette AA, Okonkwo OC, Sodhi A, Ries ML, Birdsill AC, Alexander AL, Rowley HA, Puglielli L, Asthana S, Sager MA (2012) CSF T-Tau/A β 42 predicts white matter microstructure in healthy adults at risk for Alzheimer's disease. *PLoS ONE* 7, e37720 [PubMed: 22701578]
12. McMorris FA, Dubois-Dalcq M (1988) Insulin-like growth factor I promotes cell proliferation and oligodendroglial commitment in rat glioblastoma progenitor cells developing in vitro. *Journal of Neuroscience Research*, 21 (2-4), 199–209 [PubMed: 3216421]
13. Suzuki R, Lee K, Jing E, Biddinger SB, McDonald JG, Montine TJ, Craft S, Kahn CR (2010) Diabetes and insulin in regulation of brain cholesterol metabolism. *Cell Metabolism*, 12, 567–579 [PubMed: 21109190]
14. Barres BA (2008) The Mystery and Magic of Glia: A Perspective on Their Roles in Health and Disease. *Neuron*, 60, 430–440 [PubMed: 18995817]
15. Alexander AL, Hurley SA, Samsonov AA, Adluru N, Hosseinbor A, Mossahebi P, Tromp DP, Zakszewski E, Field AS (2011) Characterization of cerebral white matter properties using quantitative magnetic resonance imaging stains. *Brain connectivity*, 1, 423–446 [PubMed: 22432902]
16. Deoni SCL, Rutt BK, Arun T, Pierpaoli C, Jones DK (2008) Gleaning multicomponent T1 and T2 information from steady-state imaging data. *Magn Reson Med*, 60, 1372–1387 [PubMed: 19025904]
17. Dean DC III, Jerskey BA, Chen K, Protas H, Thiyyagura P, Roontiva A, O'Muirheartaigh J, Dirks H, Waskiewicz N, Lehman K, Siniard AL, Turk MN, Hua X, Madsen SK, Thompson PM, Fleisher AS, Huettelman MJ, Deoni SCL, Reiman EM (2014) Brain Differences in Infants at Differential Genetic Risk for Late-Onset Alzheimer Disease: A Cross-sectional Imaging Study. *JAMA Neurol* 71, 11–22. [PubMed: 24276092]
18. Nierenberg J, Pomara N, Hoptman MJ, Sidtis JJ, Ardekani BA, Lim KO (2005) Abnormal white matter integrity in healthy apolipoprotein E epsilon4 carriers. *NeuroReport*, 16(12), 1369–1372 [PubMed: 16056141]
19. Sager MA, Hermann B, La Rue A (2005) Middle-aged children of persons with Alzheimer's disease: *APOE* genotypes and cognitive function in the Wisconsin Registry for Alzheimer's Prevention. *J Geriatr Psychiatry Neurol*, 18, 245–249 [PubMed: 16306248]
20. American Diabetes Association (2010) Diagnosis and Classification of Diabetes Mellitus. *Diabetes Care*, 33(Suppl 1), S62–S69 <http://doi.org/10.2337/dc10-S062> [PubMed: 20042775]
21. Krakauer NY, Krakauer JC (2012) A New Body Shape Index Predicts Mortality Hazard Independently of Body Mass Index. *Public Library of Science (PLOS)* doi:10.1371/journal.pone.0039504
22. Johnson SC, La Rue A, Hermann BP, et al. (2011) The Effect of *TOMM40* Poly-T length on Gray Matter Volume and Cognition in Middle-Aged Persons with *APOE* ϵ 3/ ϵ 3 Genotype. *Alzheimer's & dementia : the journal of the Alzheimer's Association*, 7(4):456–465
23. O'Bryant SE, Humphreys JD, Smith GE, Ivnik RJ, Graff-Radford NR, Petersen RC, Lucas JA (2008) Detecting dementia with the mini-mental state examination (MMSE) in highly educated individuals. *Archives of Neurology*, 65(7), 963–67 [PubMed: 18625866]
24. Deoni SCL (2009) Transverse relaxation time (T2) mapping in the brain with off-resonance correction using phase-cycled steady-state free precession imaging. *J Magn Reson Imaging*, 30(2), 411–417 [PubMed: 19629970]

25. Yarnykh VL (2007) Actual flip-angle imaging in the pulsed steady state: a method for rapid three-dimensional mapping of the transmitted radiofrequency field. *Magn Reson Med*, 57(1), 192–200 [PubMed: 17191242]
26. Deoni SCL, Matthews L, Kolind SH (2013) One component? Two components? Three? The effect of including a nonexchanging 'free' water component in multicomponent driven equilibrium single pulse observation of T1 and T2. *Magn Reson Med* 70, 147–154 [PubMed: 22915316]
27. Avants BB, Epstein CL, Grossman M, Gee JC (2008) Symmetric diffeomorphic imaging registration with cross-correlation: evaluating automated labeling of elderly and neurodegenerative brain *Med Image Anal*, 12(1), 26–41 [PubMed: 17659998]
28. Schmidt P, Gaser C, Arsic M, Buck D, Forschler A, Berthele A, Hoshi M, Ilg R, Schmid VJ, Zimmer C, Hemmer B, Muhlau M (2012) An automated tool for detection of FLAIR-hyperintense white-matter lesions in Multiple Sclerosis. *Neuroimage*, 59(4), 3774–83 [PubMed: 22119648]
29. Oishi K, Faria AV, van Zijl PCM, Mori S (2011) *MRI Atlas of Human White Matter*, Second Edition
30. Liu Y, Hu L, Ji C, Chen D, Shen X, Yang N, Yue Y, Jiang J, Hong X, Ge Q, Zuo P (2009) Effects of hormone replacement therapy on magnetic resonance imaging of brain parenchyma hyperintensities in postmenopausal women. *Acta Pharmacol Sin*, 30(7), 1065–70 [PubMed: 19575009]
31. Moran C, Beare R, Phan TG, et al. (2015) Type 2 diabetes mellitus and biomarkers of neurodegeneration. *Neurology*, 85(13), 1123–30 [PubMed: 26333802]
32. Matsuzaki T, Sasaki K, Tanizaki Y, et al. (2010) Insulin resistance is associated with the pathology of Alzheimer disease: the Hisayama study. *Neurology*, 75(9), 764–70 [PubMed: 20739649]
33. Hsu JL, Chen YL, Leu JG, Jaw FS, Lee CH, Tsai YF, Hsu YF, Bai CH, Leemans A (2012) Microstructural white matter abnormalities in type 2 diabetes mellitus: a diffusion tensor imaging study. *Neuroimage*, 59(2), 1098–1105 [PubMed: 21967726]
34. Last D, Alsop DC, Abduljalil AM, Marquis RP, de Bazelaire C, Hu K, Cavallerano J, Novak V (2007) Global and regional effects of type 2 diabetes on brain tissue volumes and cerebral vasoreactivity. *Diabetes Care*, 30(5), 1193–1199 [PubMed: 17290035]
35. Zhang Y, Cao Y, Xie Y, Liu L, Qin W, Lu S, Zhang Q (2018) Altered brain structural topological properties in type 2 diabetes patients without complications, *J Diabetes*, doi: 10.1111/1753-0407.12826. [Epub ahead of print]
36. Ryu SY, Coutu JP, Rosas HD, Salat DH (2014) Effects of insulin resistance on white matter microstructure in middle-aged and older adults. *Neurology*, 82(21), 1862–1870 [PubMed: 24771537]
37. Shafee R, Buckner RL, Fischl B (2015) Gray matter myelination of 1555 human brains using partial volume corrected MRI images. *Neuroimage*, 105, 473–85 [PubMed: 25449739]
38. Cooley SA, Cabeen RP, Laidlaw DH, et al. (2014) Posterior brain white matter abnormalities in older adults with probable mild cognitive impairment. *J Clin Exp Neuropsychol*. 37(1), 61–9 [PubMed: 25523313]
39. Lindemer ER, Greve DN, Fischl BR, Augustinack JC, Salat DH (2017) Regional staging of white matter signal abnormalities in aging and Alzheimer's disease. *Neuroimage Clin*, 14:156–65 [PubMed: 28180074]
40. Nouwen A et al. (2017) Microstructural abnormalities in white and gray matter in obese adolescents with and without type 2 diabetes. *NeuroImage: Clinical*, 16, 43–51 [PubMed: 28752059]
41. Seghier ML (2012) The angular gyrus-multiple functions and multiple subdivisions. *The Neuroscientist*, 19(1), 43–61 [PubMed: 22547530]
42. Renier LA, Anurova I, De Volder AG, Carlson S, VanMeter J, Rauschecker JP (2010) Preserved functional specialization for spatial processing in the middle occipital gyrus of the early blind. *Neuron*, 68(1), 138–148 [PubMed: 20920797]
43. Nelson TJ, Alkon DL (2005) Insulin and cholesterol pathways in neuronal function, memory and neurodegeneration. *Biochem Soc Trans*, 33(Pt 5), 1033–1036 [PubMed: 16246039]

44. Wood TC, Simmons C, Hurley SA, Vernon AC, Torres J, Dell'Acqua F, Williams SC, Cash D, nd (2016) Whole-brain ex-vivo quantitative MRI of the cuprizone mouse model PeerJ, 4, e2632 [PubMed: 27833805]
45. Ihara M, Polvikoski TM, Hall R, Slade JY, Perry RH, Oakley AE, Englund E, O'Brien JT, Ince PG, Kalaria RN (2010) Quantification of myelin loss in frontal lobe white matter in vascular dementia, Alzheimer's disease, and dementia with Lewy bodies. Acta Neuropathologica, 119(5), 579–589 [PubMed: 20091409]

Author Manuscript

Author Manuscript

Author Manuscript

Author Manuscript

STUDY IMPORTANCE QUESTIONS

- The inability to respond to insulin, known as insulin resistance (IR), has been recognized as a possible risk factor of Alzheimer's disease (AD); however, little is yet known about how insulin or IR shape the brain's underlying microstructure in humans *in vivo*.
- The results of this study indicate that both insulin and IR are negatively associated with myelin content in white matter, and positively associated in gray matter. Alterations to myelinated white matter microstructure may confer vulnerability to neurodegenerative disease, although additional study is needed.

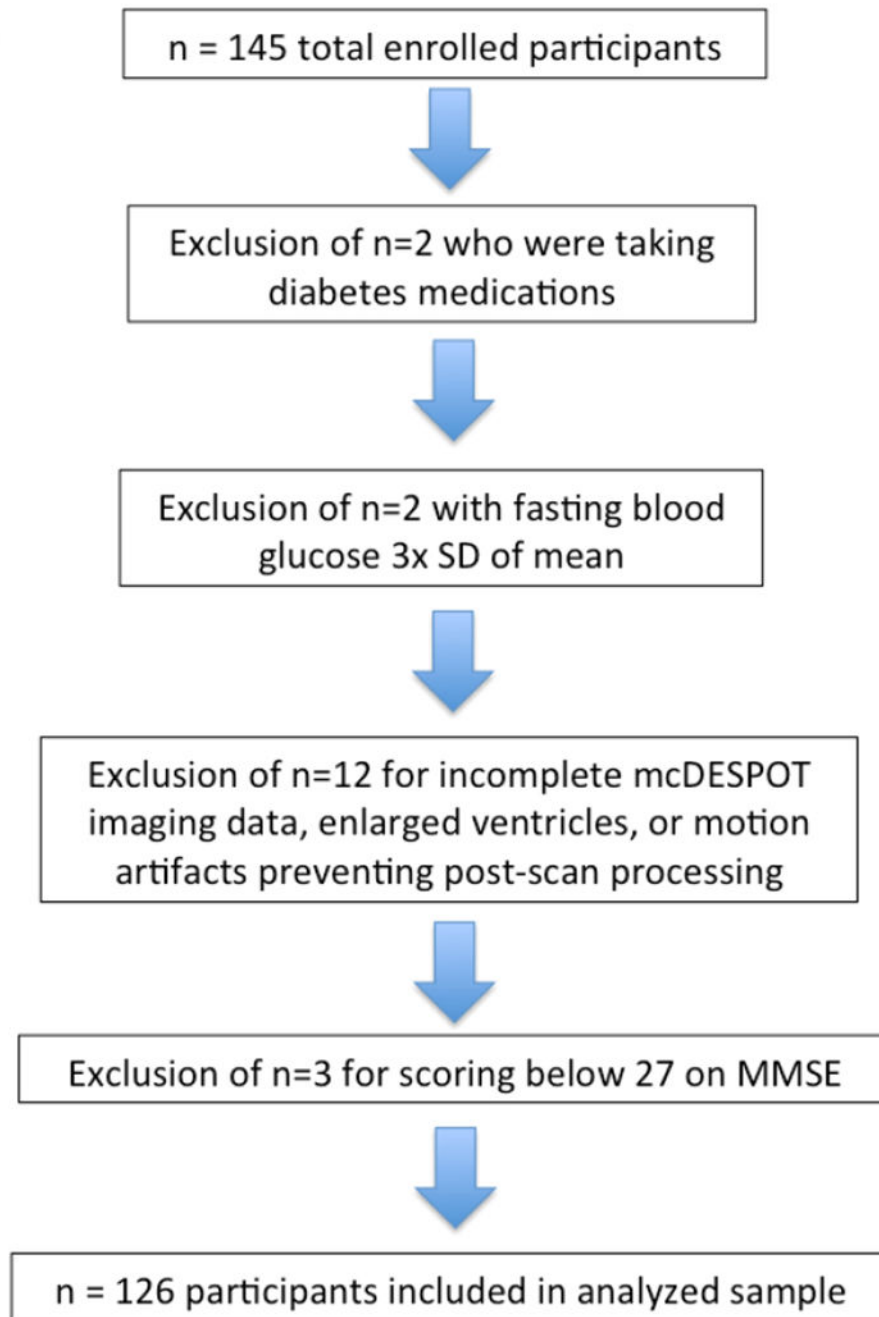


Figure 1: Participant Exclusion Flowchart

Collected data were screened for exclusionary factors. In particular, two participants were excluded for taking medications for diabetes; two participants were excluded for having fasting blood glucose levels greater than three standard deviations above the mean; and twelve participants were excluded due to incomplete mcDESPOT imaging data, enlarged ventricles, or motion artifacts which prevented post-scan processing.

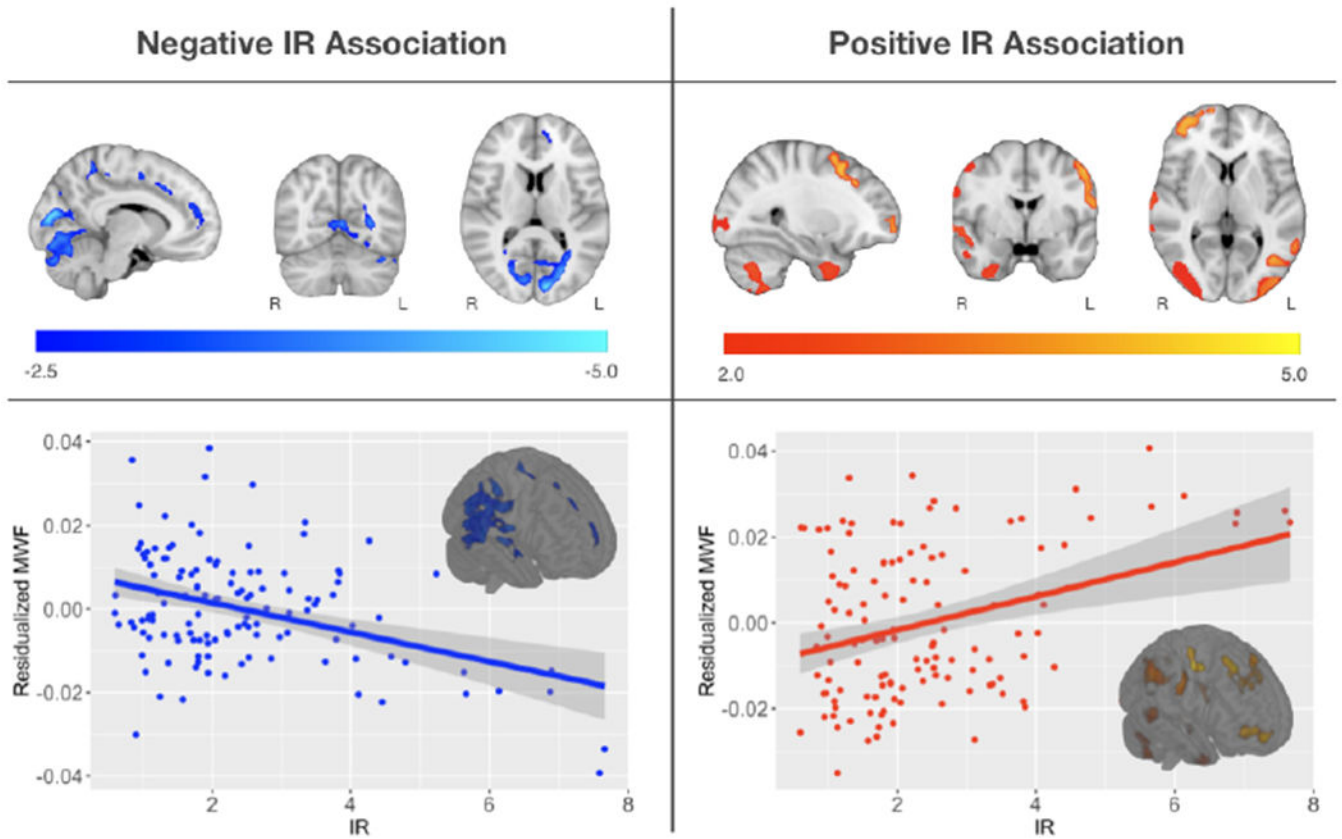


Figure 2: Main Effect of Insulin Resistance on MWF

Main Effect of Insulin Resistance on MWF- Multislice rendering of statistically significant results relating IR and MWF. Negative relationships are shown in blue and positive relationships in red, overlaid on the MNI template. For visualization, scatter plots show the overall association between mean MWF and HOMA-IR from the significant clusters. Regions where a negative association between MWF and HOMA-IR were observed localized in myelinated bilateral regions of the parieto-occipital projections of the corpus callosum and white matter surrounding the cuneus. Regions exhibiting a positive association between MWF and HOMA-IR localized in cortical regions, including frontal, occipital and temporal cortices.

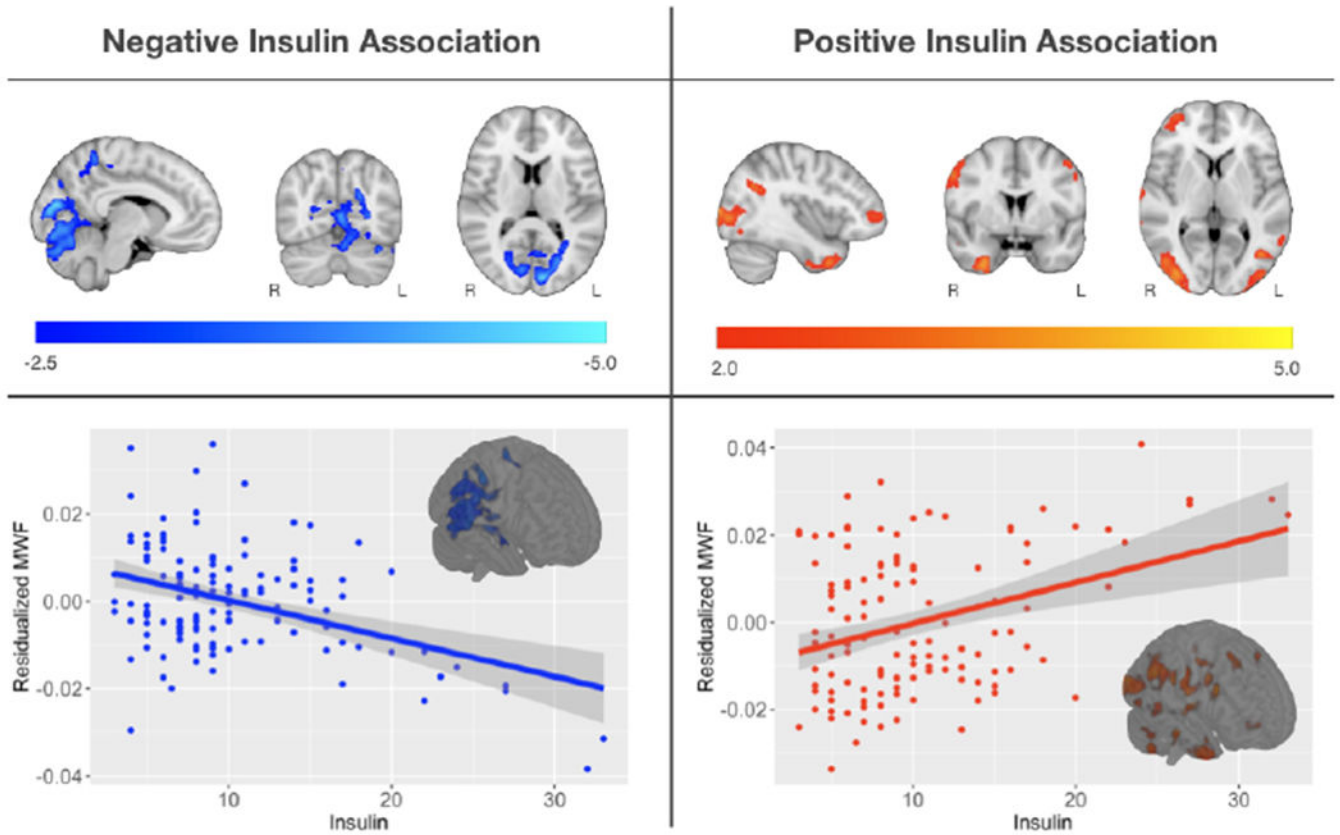


Figure 3: Main Effect of Insulin on MWF

Main Effect of Insulin on MWF- Multislice rendering of statistically significant results relating insulin and MWF. Negative relationships are shown in blue and positive relationships in red, overlaid on the MNI template. For visualization, scatter plots show the overall association between mean MWF and insulin from the significant clusters. Results were localized in similar brain regions as the associations between MWF and IR.

Table 1

Demographic, glucoregulatory, genetic, and cognitive data

	Whole Sample (n=145) Mean (SD), Range	Analysis Sample (n=126) Mean (SD), Range
Sex	96 women, 49 men	82 women, 44 men
Age (yrs)	61.4 (6.2), 45 - 74	61.5 (6.3), 45 - 74
Education (yrs)	16.9 years (2.6)	16.8 years (2.5)
Waist Circumference (cm)	96.1 (15.0), 63 - 144	95.1 (14.3), 63 - 142
Insulin	10.9 (7.6)	10.3 (5.9)
HOMA-IR (FG × FINSI) / 405	2.7 (2.8), 0.24 - 27.0	2.42 (1.5), 0.59 - 7.7
Number and Range of Days Separating MRI date and Blood Draw date	4.4 (15.9), 0 - 135	4.7 (16.7), 0 - 135
Race		
White	135	121
Black or African American	8	3
Cuban	1	1
Asian	1	1
Diabetes Status		
Normoglycemic (FG < 100 mg/dL)	111 (76.6%)	100 (79.4%)
Impaired Fasting Glucose (FG > 100mg/dL)	34 (23.4%)	26 (20.6%)
Diabetes Diagnosis	2	0
APOE ε4 genotype		
APOE ε4 (hetero- or homozygous)	56 (38.6%)	46 (36.5%)
Parental family history AD	102 (70.3%)	93 (73.8%)
Cognitive Function		
MMSE	29.3 (1.0), 25 - 30	29.4 (0.8), 27 - 30

HOMA-IR= Homeostatic Model Assessment of Insulin Resistance; FG=fasting glucose; FINSI=fasting insulin; MMSE = Mini-mental state examination; Means (std deviations).

Normoglycemic ranges determined from American Diabetes Association guidelines.

Table 2.

The association of insulin resistance on MWF in brain regions

Region	Coordinates (millimeters)	T-Value	Observed extent threshold	Cluster level p-value
IR positive direction cluster data (n=126)				
Right superior precentral region	54, 14, 30	4.29	1027	.001
Right superior temporo-parietal region	28, -102, 0	4.24	1185	.000
Right inferior temporal region	34, 12, -42	4.11	892	.001
Right superior temporo-parietal region	50, -58, 26	4.03	621	.005
Left occipito-parietal region	-22, -106, 0	4.00	509	.009
Left inferior middle region	-40, -68, 2	3.81	427	.015
Left superior temporal region	-56, -60, 22	3.74	286	.040
Right middle superior frontal region	32, 20, 58	3.73	294	.038
Left superior medial-frontal region	-52, -2, 46	3.54	405	.017
Right superior temporal region	68, -8, -2	3.60	640	.004
Right superior frontal region	24, 62, -6	3.57	398	.018
IR negative direction cluster data (n=126)				
Parieto-occipital projections of corpus callosum	-10, -84, 14	4.80	3801	.000
Cuneus White Matter	10, -76, 14	4.22	657	.004

Extent threshold (k) = 174 voxels, $p < .005$, uncorrected for positive and negative directional multiple regression analyses. All significant voxel-level p-values were less than .005.

Abbreviations: MWF = myelin water fraction; IR = insulin resistance.

Table 3.

The association of insulin on MWF in brain regions

Region	Coordinates (millimeters)	T-Value	Observed extent threshold	Cluster level p-value
Insulin positive direction cluster data (n=126)				
Right inferior frontal gyrus	54, 14, 30	4.52	911	.001
Right cuneus region	52, -60, 24	4.18	748	.002
Right inferior temporal pole region	30, 4, -42	4.10	832	.001
Right occipital region	36, -88, 6	4.08	1046	.000
Left occipital region	-40, -68, 2	3.86	427	.015
Left cuneus region	-22, -106, 0	3.85	326	.030
Right superior frontal region	32, 20, 58	3.76	323	.031
Right superior temporal gray matter region	68, -8, 0	3.57	430	.015
Insulin negative direction cluster data (n=126)				
Parietal-occipital projections of corpus callosum	-10, -84, 14	4.69	3980	.000
Cuneus white matter	10, -76, 14	4.19	556	.007
Parietal white matter	-10, -46, 56	4.04	263	.048

Extent threshold (k) = 174 voxels, $p < .005$, uncorrected for positive and negative directional multiple regression analyses. All significant voxel-level p-values were less than .005.

Abbreviation: MWF = myelin water fraction.